

# Mesonic excitations and $\pi$ – $\pi$ scattering lengths at finite temperature in the two-flavor Polyakov–Nambu–Jona-Lasinio model

Wei-jie Fu<sup>a</sup>, and Yu-xin Liu<sup>a,b,\*</sup>

<sup>a</sup> Department of Physics and State Key Laboratory of Nuclear Physics and Technology,  
Peking University, Beijing 100871, China

<sup>b</sup> Center of Theoretical Nuclear Physics, National Laboratory of Heavy Ion Accelerator,  
Lanzhou 730000, China

November 22, 2018

## Abstract

The mesonic excitations and  $s$ -wave  $\pi$ – $\pi$  scattering lengths at finite temperature are studied in the two-flavor Polyakov–Nambu–Jona-Lasinio (PNJL) model. The masses of  $\pi$  meson and  $\sigma$  meson, pion-decay constant, the pion-quark coupling strength, and the scattering lengths  $a_0$  and  $a_2$  at finite temperature are calculated in the PNJL model with two forms of Polyakov-loop effective potential. The obtained results are almost independent of the choice of the effective potentials. The calculated results in the PNJL model are also compared with those in the conventional Nambu–Jona-Lasinio model and indicate that the effect of color confinement screens the effect of temperature below the critical one in the PNJL model. Furthermore, the Goldberger-Treiman relation and the Gell-Mann–Oakes–Renner relation are extended to the case at finite temperature in the PNJL model.

**PACS Numbers:** 12.38.Aw, 11.30.Rd, 13.75.Lb, 14.40.Aq

---

\*Corresponding author, e-mail address: yxliu@pku.edu.cn

# 1 Introduction

QCD thermodynamics and phase diagram, especially about the restoration of the chiral symmetry and the deconfinement phase transition which are expected to occur in ultra-relativistic heavy-ion collisions [1–8] or in the interior of neutron stars [9–12], has been a subject of intense investigation in recent years. One significant aspect to investigate the restoration of the chiral or axial symmetry and the deconfinement phase transition is to study the variation of properties of particles propagating in hot and/or dense medium [13–15]. In this work, we focus on the influence of a hot medium on the properties of light pseudoscalar ( $\pi$ ) and scalar ( $\sigma$ ) mesons, and  $\pi$ – $\pi$  scattering lengths. Special attentions are paid to their dramatic variations near the regime where the chiral phase transition and the deconfinement phase transition occur. We expect to extract the signals of phase transition from mesonic excitations and  $\pi$ – $\pi$  interactions in the hot medium.

A promising phenomenological approach to study the low-energy processes involving the pseudoscalar and scalar mesons at zero temperature and finite temperature is the Nambu–Jona-Lasinio (NJL) model [16–21]. The most important advantage of the NJL model is that it introduces a mechanism of the dynamical breaking of chiral symmetry (due to the quark-antiquark condensate). However, the NJL model has its disadvantage, which is the lack of the description of color confinement. To include some effects of color confinement, a Polyakov-loop improved Nambu–Jona-Lasinio (PNJL) model has been developed recent years [22–30]. In the PNJL model, the Polyakov-loop as a classical field couples to quarks and thus suppresses the contributions from wrong degrees of freedom (color non-singlet) to the thermodynamics below the critical temperature. Therefore, the introduction of the Polyakov-loop represents some aspects of the color confinement, at least on the level of statistics [29]. The validity of the PNJL model has been confirmed in a series of works by confronting the PNJL results with the lattice QCD data [27, 28, 31–33]. The phase structure and thermodynamics in the PNJL model have recently been explored extensively [29, 30, 34–46], and the impact of Polyakov-loop dynamics on the chiral susceptibility or quark number susceptibility [34, 35], QCD critical endpoint [40, 41] and critical surface [42], and the color superconductivity phase transition [28, 47–49] have attracted lots of interests. Furthermore, fluctuations beyond the mean field approximation have been included in the PNJL model [50, 51], and the PNJL model has also been extended to the regime of imaginary chemical potential [52–55] and  $0 + 1$  dimensions [56], and applied to analyze the flavors of quark-gluon-plasma [57] and the isentropic trajectories on QCD phase diagram [58].

The properties of pseudoscalar and scalar mesons at finite temperature for two [14] and three [15] flavor systems have also been investigated in the PNJL model. In Ref. [14], The mesonic correlators and spectral functions for  $\pi$  and  $\sigma$  mesons were obtained. It was found

that the  $\pi$ - $\sigma$  degeneracy in the chiral symmetry restored phase was still satisfied after coupling quarks to the Polyakov-loop and the role of  $\pi$  meson as Goldstone boson was also confirmed in the PNJL model. It was also found that, although the PNJL model can not cure the problem of the conventional NJL model as for the unphysical width of the  $\sigma$  meson, the PNJL results on the decay width improved slightly the NJL ones [14]. In order to further study the broken chiral symmetry and its restoration in the mesonic sector in the PNJL model which makes the investigation of the interplay between the restoration of chiral symmetry and the deconfinement phase transition possible, it is necessary to study the Goldberger-Treiman relation [59] and the Gell-Mann–Oakes–Renner relation [60] which are direct results due to the chiral symmetry breaking. Furthermore, one of the most fundamental hadronic processes of QCD at the mesonic level, the pion-pion scattering,  $\pi + \pi \rightarrow \pi + \pi$ , at finite temperature, which provides a direct link between the theoretical formalism of chiral symmetry and experiment, also deserves to be investigated. In this work, we will then study the problems mentioned above in the PNJL model.

The paper is organized as follows. In Sec. II we simply review the formalism of the two flavor PNJL model. In Sec. III we discuss the mesonic excitations at finite temperature in the PNJL model. The dependence of the pion-decay constant, pion-quark coupling strength, and the relation between the mass of  $\sigma$  meson and that of  $\pi$  meson on the temperature are studied in the PNJL model. We also extend the Goldberger-Treiman relation and Gell-Mann–Oakes–Renner relation to a formalism which is appropriate at finite temperature. In Sec. IV we study the  $s$ -wave  $\pi$ - $\pi$  scattering lengths in the PNJL model and compare the results in the PNJL model with those in the conventional NJL. Finally, in Sec. V, we give a summary and conclusions.

## 2 The PNJL model

The Lagrangian density for the two-flavor PNJL model is given as [27]

$$\begin{aligned} \mathcal{L}_{PNJL} = & \bar{\psi} (i\gamma_\mu D^\mu - \hat{m}_0) \psi + G \left[ (\bar{\psi}\psi)^2 + (\bar{\psi}i\gamma_5 \vec{\tau}\psi)^2 \right] \\ & - \mathcal{U}(\Phi[A], \bar{\Phi}[A], T), \end{aligned} \quad (1)$$

where  $\psi = (\psi_u, \psi_d)^T$  is the quark field,

$$D^\mu = \partial^\mu - iA^\mu \quad \text{with} \quad A^\mu = \delta_0^u A^0, \quad A^0 = g\mathcal{A}_a^0 \frac{\lambda_a}{2} = -iA_4. \quad (2)$$

The gauge coupling  $g$  is combined with the SU(3) gauge field  $\mathcal{A}_a^\mu(x)$  to define  $A^\mu(x)$  for convenience and  $\lambda_a$  are the Gell-Mann matrices in color space.  $\hat{m}_0 = \text{diag}(m_u, m_d)$  is the current quark mass matrix. Throughout this work, we take  $m_u = m_d \equiv m_0$ , assuming the

isospin symmetry is reserved on the Lagrangian level. The four-fermion interaction with an effective coupling strength  $G$  for scalar and pseudoscalar channels has  $SU_V(2) \times SU_A(2) \times U_V(1)$  symmetry, which is broken to  $SU_V(2) \times U_V(1)$  when  $m_0 \neq 0$ . Here  $\tau^a$  ( $a = 1, 2, 3$ ) in the Lagrangian density (Eq. (1)) are Pauli matrices in flavor space.

The  $\mathcal{U}(\Phi, \bar{\Phi}, T)$  in the Lagrangian density is the Polyakov-loop effective potential, which controls the Polyakov-loop dynamics and can be expressed in terms of the trace of the Polyakov-loop  $\Phi = (\text{Tr}_c L)/N_c$  and its conjugate  $\bar{\Phi} = (\text{Tr}_c L^\dagger)/N_c$ . Here the Polyakov-loop  $L$  is a matrix in color space, which can be explicitly given as [27]

$$L(\vec{x}) = \mathcal{P} \exp \left[ i \int_0^\beta d\tau A_4(\vec{x}, \tau) \right] = \exp [i\beta A_4] , \quad (3)$$

where  $\beta = 1/T$  is the inverse of the temperature. The Polyakov-loop effective potential has the  $Z(3)$  center symmetry like the pure-gauge QCD Lagrangian. When the temperature is lower than a critical value ( $T_0 \simeq 270 \text{ MeV}$  in pure gauge QCD [27]), the value of  $\Phi$  (and  $\bar{\Phi}$ ) which minimizes the Polyakov-loop effective potential is zero, meaning that the phase is color confined and has the  $Z(3)$  symmetry. However, when the temperature is above the critical temperature  $T_0$ ,  $\Phi$  develops a nonzero value which minimizes the effective potential and the system is transited from a  $Z(3)$  symmetric, confined phase to a  $Z(3)$  symmetry broken, deconfined phase. The temperature dependent Polyakov-loop effective potential is chosen to reproduce the lattice data for both the expectation value of the Polyakov-loop [61] and some thermodynamic quantities [62]. In the PNJL Lagrangian in Eq. (1), the coupling between the Polyakov-loop and quarks is uniquely determined by the covariant derivative  $D_\mu$ .

In previous works, two possible forms for the Polyakov-loop effective potential have been well developed. Following our previous work [29], we denote them as  $\mathcal{U}_{\text{pol}}(\Phi, \bar{\Phi}, T)$  and  $\mathcal{U}_{\text{imp}}(\Phi, \bar{\Phi}, T)$ , respectively. The former is a polynomial in  $\Phi$  and  $\bar{\Phi}$  [27] and the latter is an improved effective potential in which the higher order polynomial terms in  $\Phi$  and  $\bar{\Phi}$  are replaced by a logarithm [28]. Both the effective potentials are taken in our work to investigate whether our results depend on the details of the Polyakov-loop effective potential. These two effective potentials have the following forms

$$\frac{\mathcal{U}_{\text{pol}}(\Phi, \bar{\Phi}, T)}{T^4} = -\frac{b_2(T)}{2} \bar{\Phi} \Phi - \frac{b_3}{6} (\Phi^3 + \bar{\Phi}^3) + \frac{b_4}{4} (\bar{\Phi} \Phi)^2 , \quad (4)$$

with

$$b_2(T) = a_0 + a_1 \left( \frac{T_0}{T} \right) + a_2 \left( \frac{T_0}{T} \right)^2 + a_3 \left( \frac{T_0}{T} \right)^3 , \quad (5)$$

and

$$\frac{\mathcal{U}_{\text{imp}}(\Phi, \bar{\Phi}, T)}{T^4} = -\frac{1}{2} A(T) \bar{\Phi} \Phi + B(T) \ln [1 - 6 \bar{\Phi} \Phi + 4(\bar{\Phi}^3 + \Phi^3) - 3(\bar{\Phi} \Phi)^2] , \quad (6)$$

with

$$A(T) = A_0 + A_1 \left( \frac{T_0}{T} \right) + A_2 \left( \frac{T_0}{T} \right)^2, \quad B(T) = B_3 \left( \frac{T_0}{T} \right)^3. \quad (7)$$

A precise fit of the parameters in these two effective potentials has been performed to reproduce some pure-gauge lattice QCD data in Refs. [27, 28]. The results are listed in Table 1, Table 2, respectively. The parameter  $T_0$  is the critical temperature for the deconfinement phase transition to take place in the pure-gauge QCD and  $T_0$  is chosen to be 270 MeV according to the lattice calculations.

Table 1: Parameters for the polynomial effective potential  $\mathcal{U}_{\text{pol}}$

$a_0$	$a_1$	$a_2$	$a_3$	$b_3$	$b_4$
6.75	-1.95	2.625	-7.44	0.75	7.5

Table 2: Parameters for the improved effective potential  $\mathcal{U}_{\text{imp}}$

$A_0$	$A_1$	$A_2$	$B_3$
3.51	-2.47	15.2	-1.75

In the NJL sector of the model, three parameters need to be determined: the three-momentum cutoff  $\Lambda$ , the current quark mass  $m_0$ , and the coupling strength  $G$ . In our work we employ the zero-temperature values of the quark condensate, pion decay constant and the mass of pion to fix the parameters. The obtained results are given in Table 3.

Table 3: Parameters of the NJL sector of the model and the physical quantities being fitted

$\Lambda$ (MeV)	$G$ (GeV $^{-2}$ )	$m_0$ (MeV)	$ \langle \bar{\psi}_u \psi_u \rangle ^{1/3}$ (MeV)	$f_\pi$ (MeV)	$m_\pi$ (MeV)
659.28	4.773	5.32	250.0	92.4	139.3

### 3 Mesonic excitations at finite temperature

Before we study the properties of mesonic excitations at finite temperature in the PNJL model, the gap equation whose solution provides the constituent mass of the quark should

be given. As presented in Ref. [14], such gap equation in the Hartree approximation reads

$$m = m_0 + 2GT \text{Tr} \sum_{n=-\infty}^{+\infty} \int_{\Lambda} \frac{d^3p}{(2\pi)^3} \frac{-1}{\not{p} - m + \gamma^0(-iA_4)}, \quad (8)$$

where the imaginary time formalism is used and the temporal component of the four-momentum is discretized, i.e.  $p_0 = i\omega_n$  and  $\omega_n = (2n+1)\pi T$  is the Matsubara frequency for a fermion;  $m$  is the constituent mass of the quark; Tr is the trace which operates over Dirac, flavor, and color spaces. Here the three-momentum cut-off is employed. After a sum of the Matsubara frequencies, Eq. (8) can be written as

$$m = m_0 + 2GN_f \sum_{c=1}^{N_c} \int_{\Lambda} \frac{d^3p}{(2\pi)^3} \frac{2m}{E_p} \{1 - f[E_p - (-iA_{4cc})] - f[E_p + (-iA_{4cc})]\}, \quad (9)$$

where  $E_p = (p^2 + m^2)^{1/2}$  and the summation over the color index can be further written as

$$\begin{aligned} & \sum_{c=1}^{N_c} f[E_p - (-iA_{4cc})] \\ = & \sum_{c=1}^{N_c} \frac{1}{e^{\beta E_p} e^{i\beta A_{4cc}} + 1} \\ = & [(e^{\beta E_p} e^{i\beta A_{422}} + 1)(e^{\beta E_p} e^{i\beta A_{433}} + 1) + (e^{\beta E_p} e^{i\beta A_{411}} + 1)(e^{\beta E_p} e^{i\beta A_{433}} + 1) \\ & + (e^{\beta E_p} e^{i\beta A_{411}} + 1)(e^{\beta E_p} e^{i\beta A_{422}} + 1)] [(e^{\beta E_p} e^{i\beta A_{411}} + 1)(e^{\beta E_p} e^{i\beta A_{422}} + 1)(e^{\beta E_p} e^{i\beta A_{433}} + 1)]^{-1} \\ = & N_c \frac{\bar{\Phi} e^{-\beta E_p} + 2\Phi e^{-2\beta E_p} + e^{-3\beta E_p}}{1 + 3\bar{\Phi} e^{-\beta E_p} + 3\Phi e^{-2\beta E_p} + e^{-3\beta E_p}} = N_c f_{\Phi}^+(E_p), \end{aligned} \quad (10)$$

where the distribution function  $f_{\Phi}^+(E_p)$  in the PNJL model has been given in Ref. [14] with another method and we follow their notations. We can find that, when  $\Phi = \bar{\Phi} = 1$ ,  $f_{\Phi}^+(E_p)$  becomes the conventional Fermi-Dirac distribution function. In the same way, the summation of the last term in Eq. (9) is

$$\begin{aligned} & \sum_{c=1}^{N_c} f[E_p + (-iA_{4cc})] \\ = & N_c \frac{\Phi e^{-\beta E_p} + 2\bar{\Phi} e^{-2\beta E_p} + e^{-3\beta E_p}}{1 + 3\Phi e^{-\beta E_p} + 3\bar{\Phi} e^{-2\beta E_p} + e^{-3\beta E_p}} = N_c f_{\Phi}^-(E_p). \end{aligned} \quad (11)$$

Finally, the gap equation is given by

$$m = m_0 + 2GN_f N_c \int_{\Lambda} \frac{d^3p}{(2\pi)^3} \frac{2m}{E_p} [1 - f_{\Phi}^+(E_p) - f_{\Phi}^-(E_p)]. \quad (12)$$

The gap equation in the PNJL model at finite temperature can also be simply derived from the gap equation at zero temperature, which is

$$m = m_0 + 8GmN_f N_c iI_1, \quad (13)$$

where

$$I_1 = \int \frac{d^4 p}{(2\pi)^4} \frac{1}{p^2 - m^2}. \quad (14)$$

To calculate the integral  $I_1$  at finite temperature in the PNJL model, we just need to replace the integral in  $p_0$  with  $iT \sum_n \frac{1}{N_c} \sum_c$  with  $p_0 = i\omega_n - iA_{4cc}$ , i.e.

$$\begin{aligned} I_1 &= iT \sum_{n=-\infty}^{+\infty} \frac{1}{N_c} \sum_{c=1}^{N_c} \int_{\Lambda} \frac{d^3 p}{(2\pi)^3} \frac{1}{(i\omega_n - iA_{4cc})^2 - E_p^2} \\ &= -i \int_{\Lambda} \frac{d^3 p}{(2\pi)^3} \frac{1}{2E_p} [1 - f_{\Phi}^+(E_p) - f_{\Phi}^-(E_p)]. \end{aligned} \quad (15)$$

We have shown that calculations at finite temperatures in the PNJL model can be simply derived from calculations at zero temperature above. Therefore, in the following we investigate the mesonic excitations at finite temperature in the PNJL model starting from those at zero temperature. We follow the formalism in Ref. [18] and the  $\pi$  and  $\sigma$  mesons correspond to the pseudoscalar isovector modes and the scalar isoscalar mode, respectively. For the pseudoscalar modes, defining the operators

$$\tau^{\pm} = \frac{1}{\sqrt{2}}(\tau_1 \pm i\tau_2), \quad (16)$$

we can reexpress the four-fermion term in the pseudoscalar channel in the Lagrangian in Eq. (1) as

$$(\bar{\psi} i\gamma_5 \vec{\tau} \psi)^2 = 2 (\bar{\psi} i\gamma_5 \tau^+ \psi) (\bar{\psi} i\gamma_5 \tau^- \psi) + (\bar{\psi} i\gamma_5 \tau_3 \psi) (\bar{\psi} i\gamma_5 \tau_3 \psi). \quad (17)$$

The effective interaction resulting from the exchange of a  $\pi$  meson can be obtained as an infinite sum of loops in the random-phase approximation (RPA) [18] and the leading order terms in  $N_c$  is shown diagrammatically in Fig. 1.

$$= i\gamma_5 T_i \frac{-ig_{\pi qq}^2}{k^2 - m_{\pi}^2} i\gamma_5 T_j$$

Figure 1: Schematic representation of the effective interaction for the pseudoscalar modes in the RPA, where the double dashed line represents the effective propagator of  $\pi$  mesons and the solid lines are quark lines; the black dots denote the effective coupling between  $\pi$  meson and quarks. Here,  $T_i = T_j = \tau_3$  for  $\pi^0$ , and  $T_i = \tau^{\pm}$ ,  $T_j = \tau^{\mp}$  for  $\pi^{\pm}$ .

Using the symbols in Ref. [18], the left hand side of the equation in Fig. 1 can be denoted as  $iU_{ij}(k^2)$ . Summing up all the terms on the right-hand side, we obtain

$$iU_{ij}(k^2) = i\gamma_5 T_i \frac{2iG}{1 - 2G\Pi_{ps}(k^2)} i\gamma_5 T_j. \quad (18)$$

Comparing Eq. (18) with the equation in Fig. 1, one can find that the mass of  $\pi$  mesons is related to the pole of Eq. (18), which is the solution of the following equation [18]

$$1 - 2G\Pi_{ps}(k^2) = 0. \quad (19)$$

Furthermore, the coupling strength between  $\pi$  meson and quarks  $g_{\pi qq}$  can be obtained as

$$g_{\pi qq}^2 = \left[ \frac{\partial \Pi_{ps}(k^2)}{\partial k^2} \right]^{-1} \Big|_{k^2=m_\pi^2}. \quad (20)$$

Therefore, the information of  $\pi$  mesons is included in the pseudoscalar polarization  $\Pi_{ps}(k^2)$ , which reads

$$-i\Pi_{ps}(k^2) = - \int \frac{d^4 p}{(2\pi)^4} \text{Tr} [i\gamma_5 T_i iS(k+p) i\gamma_5 T_j iS(p)], \quad (21)$$

where  $iS(p) = i/(\not{p} - m)$  is the propagator of quarks. After calculating the trace in Eq. (21), one has

$$\begin{aligned} -i\Pi_{ps}(k^2) &= 4N_c N_f \int \frac{d^4 p}{(2\pi)^4} \frac{1}{p^2 - m^2} - 2N_c N_f k^2 \int \frac{d^4 p}{(2\pi)^4} \frac{1}{(p^2 - m^2)[(k+p)^2 - m^2]} \\ &= 4N_c N_f I_1 - 2N_c N_f k^2 I(k), \end{aligned} \quad (22)$$

where we have used the function  $I_1$  given in Eq. (14) and also defined the function  $I(k)$  with the same symbols as used in Refs. [18, 63, 64], i.e.

$$I(k) = \int \frac{d^4 p}{(2\pi)^4} \frac{1}{(p^2 - m^2)[(k+p)^2 - m^2]}. \quad (23)$$

Furthermore, we introduce another two functions as done in Refs. [63, 64], which will be used in the following:

$$K(k) = \int \frac{d^4 p}{(2\pi)^4} \frac{1}{(p^2 - m^2)^2[(k+p)^2 - m^2]}, \quad (24)$$

$$L(k) = \int \frac{d^4 p}{(2\pi)^4} \frac{1}{(p^2 - m^2)^2[(k+p)^2 - m^2]^2}. \quad (25)$$

Then, substituting the expression of the pseudoscalar polarization in Eq. (22) into Eq. (19), we have

$$1 - 8GN_c N_f iI_1 + 4GN_c N_f k^2 iI(k) = 0. \quad (26)$$



Upon inserting the gap equation (in Eq. (13)) into the above equation, one obtains [18]

$$\frac{m_0}{m} + 4GN_c N_f k^2 i I(k) = 0, \quad (27)$$

whose solution gives the mass of the pseudoscalar mode. The explicit expression for the coupling between  $\pi$  meson and quarks can be easily obtained upon substituting Eq. (22) into Eq. (20), and, in turn, it reads [63]

$$g_{\pi qq}^2 = \frac{i}{N_c N_f} \frac{1}{I(m_\pi) + I(0) - m_\pi^2 K(m_\pi)}. \quad (28)$$

In the case of finite temperature in the PNJL model, we need to extend the function  $I(k)$  in the same way as taken for the function  $I_1$ . When the three momentum is vanishing, i.e.  $k = (\omega, 0)$ ,  $I(\omega, 0)$  at finite temperature in the PNJL model is

$$I(\omega, 0) = -i \int_{\Lambda} \frac{d^3 p}{(2\pi)^3} \frac{1}{E_p(\omega^2 - 4E_p^2)} [1 - f_{\Phi}^+(E_p) - f_{\Phi}^-(E_p)]. \quad (29)$$

Then Eq. (27) at finite temperature can be rewritten as

$$\frac{m_0}{m} + 4GN_c N_f m_\pi^2 \int_{\Lambda} \frac{d^3 p}{(2\pi)^3} \frac{1}{E_p(m_\pi^2 - 4E_p^2)} [1 - f_{\Phi}^+(E_p) - f_{\Phi}^-(E_p)] = 0. \quad (30)$$

Furthermore, we have

$$K(\omega, 0) = i \int_{\Lambda} \frac{d^3 p}{(2\pi)^3} \frac{\omega^2 - 12E_p^2}{4E_p^3(\omega^2 - 4E_p^2)^2} [1 - f_{\Phi}^+(E_p) - f_{\Phi}^-(E_p)], \quad (31)$$

$$L(\omega, 0) = i \int_{\Lambda} \frac{d^3 p}{(2\pi)^3} \frac{\omega^2 - 20E_p^2}{2E_p^3(\omega^2 - 4E_p^2)^3} [1 - f_{\Phi}^+(E_p) - f_{\Phi}^-(E_p)]. \quad (32)$$

In the same way, properties of  $\sigma$  mesons can be extracted from the scalar polarization  $\Pi_s(k^2)$ , which is

$$\begin{aligned} -i\Pi_s(k^2) &= - \int \frac{d^4 p}{(2\pi)^4} \text{Tr} [iS(k+p)iS(p)] \\ &= 4N_c N_f I_1 - 2N_c N_f (k^2 - 4m^2) I(k). \end{aligned} \quad (33)$$

Therefore, employing the RPA approximation for the scalar channel in the same procedure as for the effective interaction in the pseudoscalar channel, one could determine the mass of  $\sigma$  meson which is the pole of its corresponding effective propagator, i.e.  $1 - 2G\Pi_s(m_\sigma^2) = 0$ , explicitly given by

$$\frac{m_0}{m} + 4GN_c N_f (m_\sigma^2 - 4m^2) i I(m_\sigma) = 0. \quad (34)$$

The relation between the mass of  $\sigma$  meson and that of  $\pi$  meson could be obtained by comparing Eq. (34) and Eq. (27) as

$$m_\sigma^2 = 4m^2 + m_\pi^2 \frac{I(m_\pi)}{I(m_\sigma)}, \quad (35)$$

which returns to the relation given in Ref. [18] when the difference between  $I(m_\pi)$  and  $I(m_\sigma)$  is neglected.

In the following, we would investigate the pion-decay constant  $f_\pi$  at finite temperature in the PNJL model with a starting of the definition of  $f_\pi$

$$\langle 0 | J_{5\mu}^i(x) | \pi^j \rangle = i k_\mu f_\pi \delta^{ij}. \quad (36)$$

Considering the explicit expression of the left hand side in the PNJL model

$$\langle 0 | J_{5\mu}^i(x) | \pi^j \rangle = - \int \frac{d^4 p}{(2\pi)^4} \text{Tr} \left[ i \gamma_\mu \gamma_5 \frac{\tau^i}{2} i S(k+p) i g_{\pi qq} \gamma_5 \tau^j i S(p) \right], \quad (37)$$

we arrive at

$$f_\pi = -4i N_c g_{\pi qq} m I(m_\pi). \quad (38)$$

Employing the expression of the pion-quark coupling in Eq. (28) and considering the fact  $N_f = 2$  in the present case, one has [63]

$$f_\pi^2 = -8i N_c m^2 \frac{I^2(m_\pi)}{I(0) + I(m_\pi) - m_\pi^2 K(m_\pi)}, \quad (39)$$

and

$$f_\pi^2 g_{\pi qq}^2 = 4m^2 \frac{I^2(m_\pi)}{[I(0) + I(m_\pi) - m_\pi^2 K(m_\pi)]^2} \equiv m^2 r^2, \quad (40)$$

where we have defined a symbol  $r$  as

$$r \equiv \frac{2I(m_\pi)}{I(0) + I(m_\pi) - m_\pi^2 K(m_\pi)}. \quad (41)$$

When the temperature is approaching zero,  $I(m_\pi) \approx I(0)$ ,  $K(m_\pi) \approx 0$ ,  $r \rightarrow 1$ . Eq. (40) returns then to the quark level version of the Goldberger-Treiman relation at zero temperature [59]. As we show below, when the temperature is near some critical temperature,  $r$  deviates from 1 evidently. Furthermore, from Eq. (27), one has the mass of  $\pi$  meson as

$$m_\pi^2 = -\frac{m_0}{m} \frac{1}{4G N_c N_f i I(m_\pi)}. \quad (42)$$

One may also combine this equation with Eq. (39). It gives consequently

$$m_\pi^2 f_\pi^2 = \frac{m_0 m}{G} \frac{I(m_\pi)}{I(0) + I(m_\pi) - m_\pi^2 K(m_\pi)}. \quad (43)$$

And the constituent mass of the quark  $m$  is related with the condensate of quark by

$$\begin{aligned} m &= -2GN_f\langle\bar{u}u\rangle + m_0 \\ &= -2G\langle\bar{\psi}\psi\rangle + m_0. \end{aligned} \quad (44)$$

Replacing the constituent mass in Eq. (43) with the quark condensate in Eq. (44), we obtain

$$m_\pi^2 f_\pi^2 = -m_0\langle\bar{\psi}\psi\rangle r + \frac{m_0^2}{2G}r = -m_0\langle\bar{\psi}\psi\rangle r \left[1 + \frac{m_0}{2G|\langle\bar{\psi}\psi\rangle|}\right]. \quad (45)$$

As mentioned above, at zero temperature  $r \rightarrow 1$ . Considering the lowest-order contribution in  $m_0$ , one obtains then  $m_\pi^2 f_\pi^2 \simeq -m_0\langle\bar{\psi}\psi\rangle$ , which is the lowest-order approximation to the Gell-Mann–Oakes–Renner relation [60].

Before our numerical calculations, we need to give the equations to determine the values of the Polyakov-loop  $\Phi$  and its conjugate  $\bar{\Phi}$ . In the mean-field approximation or equivalently the Hartree approximation, the thermodynamical potential density for the Lagrangian density in Eq. (1) is given as [14]

$$\begin{aligned} \Omega(\Phi, \bar{\Phi}, m, T) &= \frac{(m_0 - m)^2}{4G} + \mathcal{U}(\Phi, \bar{\Phi}, T) - 2N_f N_c \int_\Lambda \frac{d^3p}{(2\pi)^3} E_p \\ &\quad - 2N_f T \int_\Lambda \frac{d^3p}{(2\pi)^3} \left[ \ln(1 + N_c \bar{\Phi} e^{-\beta E_p} + N_c \Phi e^{-2\beta E_p} + e^{-3\beta E_p}) \right. \\ &\quad \left. + \ln(1 + N_c \Phi e^{-\beta E_p} + N_c \bar{\Phi} e^{-2\beta E_p} + e^{-3\beta E_p}) \right]. \end{aligned} \quad (46)$$

Minimizing this thermodynamical potential with respect to  $\Phi$  and  $\bar{\Phi}$ , we obtain equations

$$\frac{\partial \Omega}{\partial \Phi} = 0, \quad \frac{\partial \Omega}{\partial \bar{\Phi}} = 0. \quad (47)$$

In the absence of chemical potential, these two equations are identical, and so  $\Phi = \bar{\Phi}$  [27]. In the same way, Minimizing the thermodynamical potential in Eq. (46) with respect to the value of the constituent quark mass  $m$ , the gap equation in Eq. (12) can also be obtained.

In the following, we present our numerical results. First of all, we give our calculated values for several characteristic temperatures. These characteristic temperatures include the pseudo-transition temperature for chiral crossover,  $T_\chi$ , corresponding to the maximum of  $-dm/dT$  [14, 27, 29], the pseudo-transition temperature for deconfinement crossover,  $T_P$ , corresponding to the maximum of  $d\Phi/dT$ , the Mott temperature  $T_M$  for  $\pi$  meson, defined by

$$m_\pi(T_M) = 2m(T_M), \quad (48)$$

meaning that the pion can dissociate into a constituent quark and an antiquark above the Mott temperature, and the dissociation temperature for  $\sigma$  meson  $T_d^\sigma$  [64], defined by

$$m_\sigma(T_d^\sigma) = 2m_\pi(T_d^\sigma). \quad (49)$$

These characteristic temperatures except for  $T_P$ , can also serve in the conventional NJL model. Numerical results for these characteristic temperatures in the PNJL model with two Polyakov-loop effective potentials are shown in Table 4. Here, for comparison we also list the results in the conventional NJL model.

Table 4: Several critical temperatures in the conventional NJL model and the PNJL model with two Polyakov-loop effective potentials ( $T_0 = 270$  MeV is chosen for these two effective potentials).

	$T_\chi$ (MeV)	$T_P$ (MeV)	$T_M$ (MeV)	$T_d^\sigma$ (MeV)
PNJL ( $\mathcal{U}_{\text{pol}}$ )	253.2	245.4	264.6	253.0
PNJL ( $\mathcal{U}_{\text{imp}}$ )	245.0	232.0	259.6	246.3
NJL	184.4	—	201.2	181.9

In Fig. 2 we illustrate our calculated results of the masses of  $\pi$  and  $\sigma$  mesons, the mass of constituent quark, and the Polyakov-loop as functions of the temperature. Fig. 2 shows evidently that at a temperature not very high, the masses of the constituent quark, the pion and the  $\sigma$  mesons maintain the same as the corresponding one at zero temperature. As the temperature is around the critical one, these masses vary abruptly. And further, if the temperature is very high, the masses of  $\pi$  and  $\sigma$  mesons become degenerate, which indicates that the chiral symmetry is restored at high temperature. Such a feature is consistent with that given in the framework of Bethe-Salpeter equation combining with the Dyson-Schwinger equations (see for example Ref. [65]). We also find that two different Polyakov-loop effective potentials do not result in qualitative differences but only slightly quantitative deviations as the left panel of Fig. 2 shows. Furthermore, looking through the right panel of Fig. 2, we can notice that the chiral phase transition occurs at relatively lower temperature in the conventional NJL model.

In order to compare the obtained results in the PNJL model with those in the conventional NJL model more conveniently, we scale the temperature in unit of Mott temperature  $T_M$  and re-display the results in Fig. 3. One can recognize that, in the PNJL model, only when the temperature is very near the phase transition temperature, masses of mesons and constituent quark begin to deviate from their values at zero temperature obviously. While in the conventional NJL model, these masses begin to deviate from their zero-temperature values at much lower temperature, about  $0.4 T_M$ . This phenomenon can be attributed to the fact that, in the low temperature, chiral symmetry is broken and the quark and antiquark are in the confined hadronic phase in the PNJL model, contributions from thermal excitations of one and two quarks or antiquarks are suppressed as the distribution functions in Eq. (10)

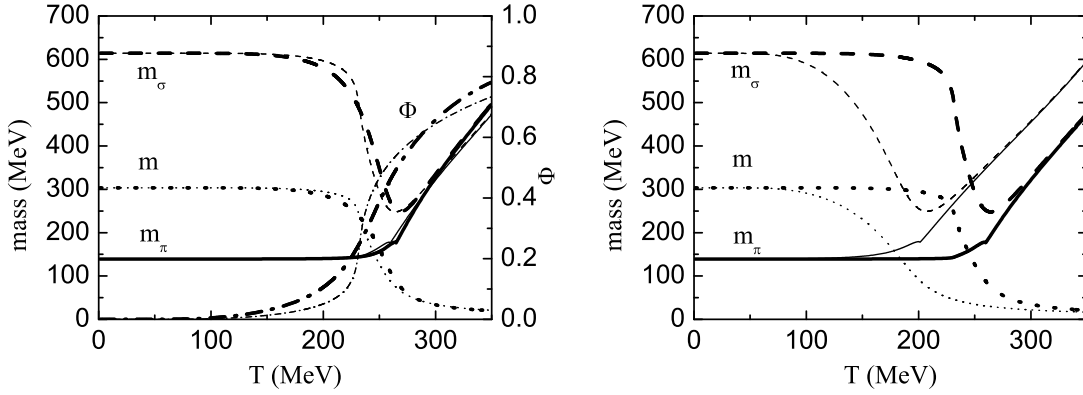


Figure 2: Left panel: calculated masses of  $\pi$  meson,  $\sigma$  meson, constituent quark and the Polyakov-loop as functions of the temperature. Here, thick curves and thin curves correspond to the results with the polynomial Polyakov-loop effective potential  $\mathcal{U}_{\text{pol}}$ , the improved effective potential  $\mathcal{U}_{\text{imp}}$ , respectively. Right panel: masses of  $\pi$ ,  $\sigma$ , and  $m$  as functions of the temperature in the PNJL model with  $\mathcal{U}_{\text{imp}}$  (thick curves) and in the conventional NJL model (thin curves).

and Eq. (11) show when the Polyakov-loop  $\Phi$  approaches zero. This is a manifestation of color confinement on the level of statistics. While in the conventional NJL model, due to the lack of the appearance of color confinement, contributions from one and two quarks or antiquarks become significant even at low temperature, which results in the phenomenon mentioned above.

In Fig. 4 we show the square of the pion-quark coupling strength  $g_{\pi qq}^2$  and the pion-decay constant  $f_\pi$  as functions of the temperature in unit of Mott temperature in the PNJL model with polynomial and improved effective potentials and in the conventional NJL model. As Eq. (31) shows, when temperature approaches the Mott temperature  $T_M$  from below, i.e. when the mass of  $\pi$  meson is about twice mass of the constituent quark,  $iK(m_\pi) \rightarrow \infty$ . Therefore, the pion-quark coupling strength and pion-decay constant vanish at  $T_M$ , as Eq. (28) and Eq. (39) show. Furthermore, One can also find in Fig. 4 that, in the PNJL model,  $g_{\pi qq}^2$  and  $f_\pi$  almost keep invariant with the increase of the temperature when the temperature is not high and these two quantities decrease rapidly only when the temperature is above  $0.8 T_M$ . While in the conventional NJL model these two quantities begin to decrease at about  $0.4 T_M$ . This behavior is also due to the lack of the color confinement in the conventional NJL model as the same as the behavior of masses of mesons and constituent

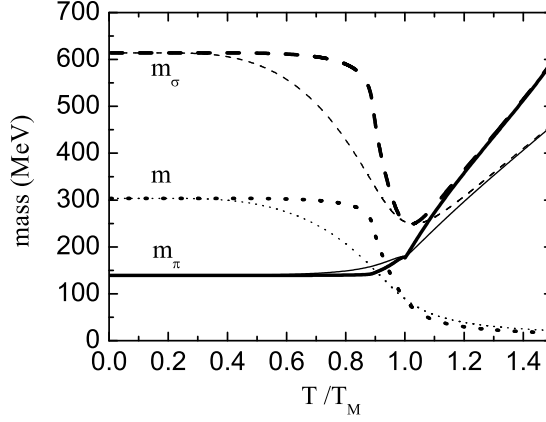


Figure 3: Calculated masses of  $\pi$  meson,  $\sigma$  meson, and constituent quark as functions of the temperature in unit of Mott temperature  $T_M$  in the PNJL model with  $\mathcal{U}_{\text{imp}}$  (thick lines) and in the conventional NJL model (thin lines).

quark as functions of temperature shown in Fig. 3.

We have shown above that the Goldberger-Treiman relation and Gell-Mann–Oakes–Renner relation at finite temperature are different from those at zero temperature in that a factor  $r$  defined in Eq. (41) is introduced. The calculated behavior of  $r$  as function of temperature is displayed in Fig. 5 and one can find that, when the temperature is below  $0.9 T_M$ ,  $r$  is almost a constant very near 1, which indicates that these two important relations at vacuum still serve well in the large region of temperature  $0 \sim 0.9 T_M$ . However, when the temperature is above  $0.9 T_M$ ,  $r$  decreases very rapidly and vanishes at  $T = T_M$ . In the region of the temperature  $0.9 T_M \sim T_M$ , the Goldberger-Treiman relation and Gell-Mann–Oakes–Renner relation at vacuum should be extended to Eq. (40), Eq. (45), respectively.

## 4 $\pi$ – $\pi$ scattering lengths

The formalism of  $s$ -wave  $\pi$ – $\pi$  scattering lengths at zero temperature in the conventional NJL model has been established in Refs. [63, 66, 67], and it has been extended to the case at finite temperature by Quack et al. [64]. In this work we follow the notation and calculation given in Ref. [63]. The invariant amplitude of  $\pi$ – $\pi$  scattering has the form:

$$\langle cp_c; dp_d | i\mathcal{M} | ap_a; bp_b \rangle = iA(s, t, u)\delta_{ab}\delta_{cd} + iB(s, t, u)\delta_{ac}\delta_{bd} + iC(s, t, u)\delta_{ad}\delta_{bc}, \quad (50)$$

where  $a$ ,  $b$ ,  $c$ , and  $d$  are the isospin labels, and  $s$ ,  $t$  and  $u$  are the Mandelstam variables,  $s = (p_a + p_b)^2$ ,  $t = (p_a - p_c)^2$  and  $u = (p_a - p_d)^2$ . The amplitude of definite total isospin  $I$ ,

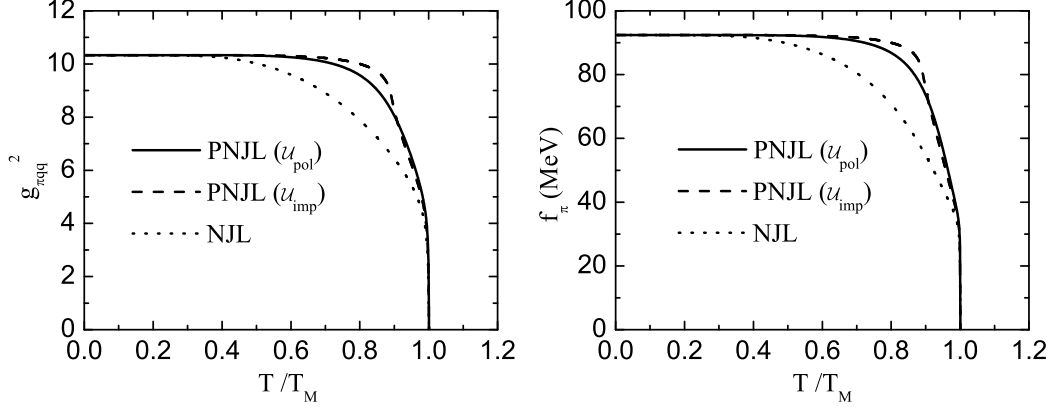


Figure 4: Left panel: calculated results of the square of the pion-quark coupling strength  $g_{\pi qq}^2$  (in Eq. (28)) as a function of the temperature in unit of Mott temperature  $T_M$  in the PNJL and the conventional NJL model. Right panel: calculated results of the pion-decay constant  $f_\pi$  (in Eq. (38)) as a function of the temperature in unit of Mott temperature.

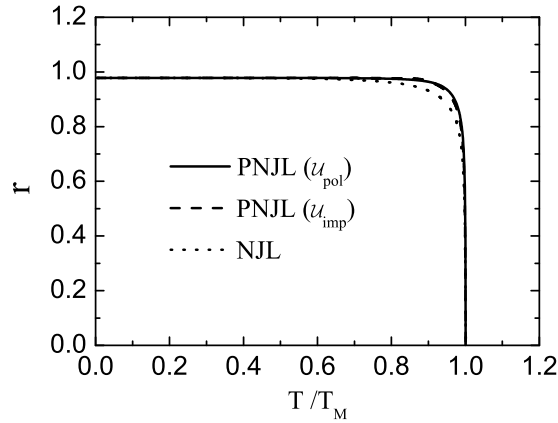


Figure 5: Calculated factor  $r$  defined in Eq. (41) as a function of the temperature in unit of Mott temperature in the PNJL and the conventional NJL model.

defined by  $A_I$ , can be projected out, given by Ref. [63]

$$A_0 = 3A + B + C, \quad A_1 = B - C, \quad \text{and} \quad A_2 = B + C. \quad (51)$$

When the scattering is at the kinematic threshold, we obtain the scattering lengths, i.e.

$$a_I = \frac{1}{32\pi} A_I(s = 4m_\pi^2, t = 0, u = 0). \quad (52)$$

For simplicity, the pion momenta can be chosen as

$$p_a = p_b = p_c = p_d = p, \quad \text{and} \quad p^2 = m_\pi^2, \quad (53)$$

which can be verified to fulfill the threshold condition in Eq. (52). To lowest order in  $1/N_c$ , there are two types of Feynman diagrams contributing to the  $s$ -wave  $\pi$ - $\pi$  scattering [63, 66], i.e. the box diagram and the  $\sigma$ -propagation diagram. Here we also present them in Fig. 6. The three diagrams in the first row of Fig. 6 are the box diagrams and the ones in the second row are the  $\sigma$ -propagation diagrams.

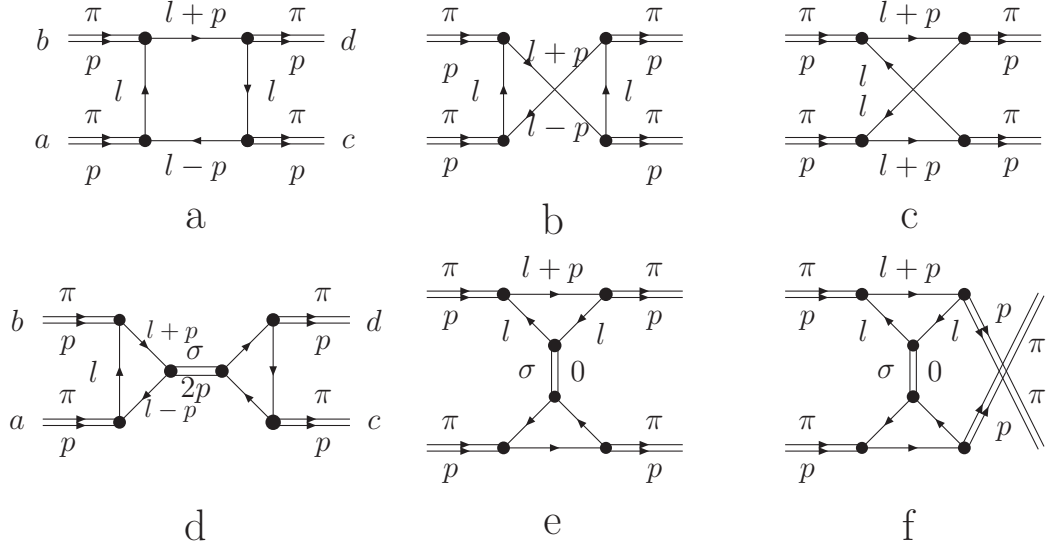


Figure 6: Feynman diagrams contributing to the  $s$ -wave  $\pi$ - $\pi$  scattering (see also Ref. [63, 66]). Here the external momenta for pions are chosen to be the special case in Eq. (53).

Following the calculation of Ref. [63], we obtain respective amplitude for each diagram



in Fig. 6 as

$$\begin{aligned} i\mathcal{M}_a &= (\delta_{ab}\delta_{cd} + \delta_{ac}\delta_{bd} - \delta_{ad}\delta_{bc})(-4N_cN_f g_{\pi qq}^4)[I(0) + I(p) - p^2 K(p)] \\ &\equiv (\delta_{ab}\delta_{cd} + \delta_{ac}\delta_{bd} - \delta_{ad}\delta_{bc})iT_a, \end{aligned} \quad (54)$$

$$\begin{aligned} i\mathcal{M}_b &= (\delta_{ab}\delta_{cd} - \delta_{ac}\delta_{bd} + \delta_{ad}\delta_{bc})(-4N_cN_f g_{\pi qq}^4)[I(0) + I(p) - p^2 K(p)] \\ &\equiv (\delta_{ab}\delta_{cd} - \delta_{ac}\delta_{bd} + \delta_{ad}\delta_{bc})iT_b, \end{aligned} \quad (55)$$

$$\begin{aligned} i\mathcal{M}_c &= (-\delta_{ab}\delta_{cd} + \delta_{ac}\delta_{bd} + \delta_{ad}\delta_{bc})(-8N_cN_f g_{\pi qq}^4) \left[ I(0) + \frac{p^4}{2}L(p) - 2p^2 K(p) \right] \\ &\equiv (-\delta_{ab}\delta_{cd} + \delta_{ac}\delta_{bd} + \delta_{ad}\delta_{bc})iT_c, \end{aligned} \quad (56)$$

$$\begin{aligned} i\mathcal{M}_d &= \delta_{ab}\delta_{cd}(8N_cN_f g_{\pi qq}^4) \frac{I^2(p)}{\left(1 - \frac{p^2}{m^2}\right) I(2p) + \frac{m_\pi^2}{4m^2} I(m_\pi)} \\ &\equiv \delta_{ab}\delta_{cd}iT_d, \end{aligned} \quad (57)$$

$$\begin{aligned} i\mathcal{M}_e &= \delta_{ac}\delta_{bd}(8N_cN_f g_{\pi qq}^4) \frac{[I(0) - p^2 K(p)]^2}{I(0) + \frac{m_\pi^2}{4m^2} I(m_\pi)} \\ &\equiv \delta_{ac}\delta_{bd}iT_e, \end{aligned} \quad (58)$$

$$\begin{aligned} i\mathcal{M}_f &= \delta_{ad}\delta_{bc}(8N_cN_f g_{\pi qq}^4) \frac{[I(0) - p^2 K(p)]^2}{I(0) + \frac{m_\pi^2}{4m^2} I(m_\pi)} \\ &\equiv \delta_{ad}\delta_{bc}iT_f. \end{aligned} \quad (59)$$

From above equations, one can notice  $T_b = T_a$ , and  $T_f = T_e$ . Substituting Eqs. (54)—(59) into Eq. (50), one obtains

$$A = 2T_a - T_c + T_d, \quad B = C = T_c + T_e. \quad (60)$$

Therefore, employing Eq. (51) we have

$$\begin{aligned} A_0 &= 6T_a - T_c + 3T_d + 2T_e, \\ A_1 &= 0, \\ A_2 &= 2(T_c + T_e). \end{aligned} \quad (61)$$

In Fig. 7 we present our calculated results of the scattering amplitudes  $T_a$ ,  $T_c$ ,  $T_d$ , and  $T_e$  as functions of the temperature in unit of  $T_M$  in the PNJL model with polynomial Polyakov-loop effective potential and improved effective potential and in the conventional NJL model. The results of the conventional NJL model in our work are roughly consistent with those given in Ref. [64]. However, there exists a difference which reads that our present calculation indicates that the scattering amplitude  $T_a$  approaches zero at the Mott temperature  $T_M$ , the calculation in Ref. [64] gives that  $T_a$  is divergent at  $T_M$ . Recalling the analysis above, we

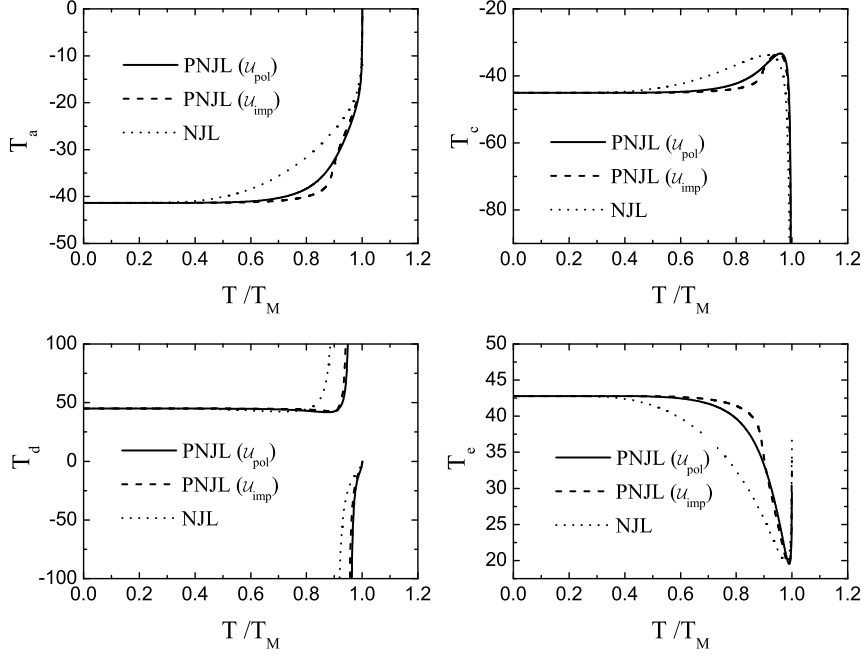


Figure 7: Calculated scattering amplitudes  $T_a$ ,  $T_c$ ,  $T_d$ , and  $T_e$  as functions of the temperature in unit of Mott temperature in the PNJL and the conventional NJL models.

would emphasized that, when the temperature approaches to  $T_M$ ,  $iK(m_\pi)$  in Eq. (31) and  $iL(m_\pi)$  in Eq. (32) are divergent and the degree of divergence of  $iL(m_\pi)$  is higher than that of  $iK(m_\pi)$ . Substituting the expression of the coupling between  $\pi$  meson and quarks  $g_{\pi qq}^2$  in Eq. (28) into Eq. (54), we find  $T_a \propto 1/(-iK(m_\pi))$  when the temperature is near the Mott temperature, therefore,  $T_a$  approaches zero at  $T_M$ . In the same way, we find that  $T_d$  approaches zero,  $T_c$  is divergent, and  $T_e$  approaches a finite value at the Mott temperature. Furthermore, when the temperature is equal to the dissociation temperature of  $\sigma$  meson, i.e.  $T = T_d^\sigma$ , we have  $m_\sigma = 2m_\pi$ , which results in that the  $\sigma$  propagator in diagram d of Fig. 6 and also the amplitude  $T_d$  (see Fig. 7) are divergent at  $T_d^\sigma$ . Comparing the results of the PNJL model with those of the conventional NJL model, one can also recognize the similar behavior as obtained previously, which reads that the  $T$ -matrix amplitudes calculated in the PNJL model deviate from their values at zero temperature only when the temperature is near the critical temperature, while the deviation occurs much earlier in the conventional NJL model. Taking amplitude  $T_d$  for example, since the mass of  $\sigma$  meson decreases with the increase of the temperature much earlier in the conventional NJL model than that in the PNJL model, as Fig. 3 shows, we expect that the divergence in  $T_d$  also occurs earlier

in the conventional NJL model, which is verified in Fig. 7. In addition, we find that the value of  $T_d^\sigma/T_M$  calculated in the conventional NJL model is about 0.90, smaller than 0.96 in the PNJL model with polynomial effective potential, and 0.95 in the PNJL model with improved effective potential.

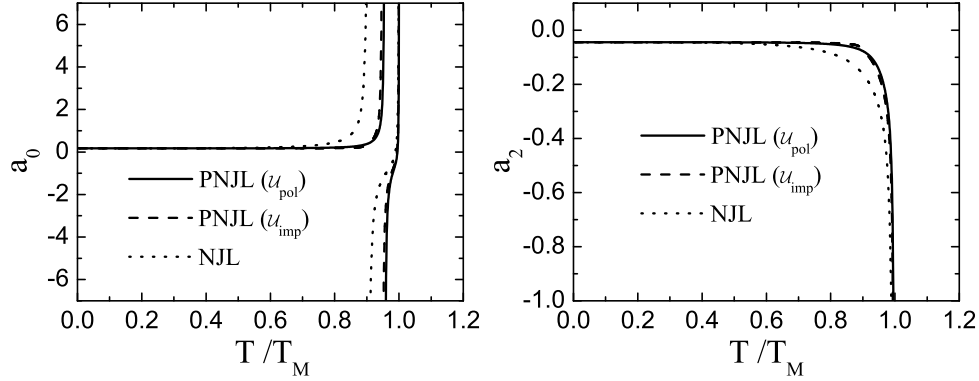


Figure 8: Calculated  $s$ -wave  $\pi$ - $\pi$  scattering lengths  $a_0$  and  $a_2$  as functions of the temperature in unit of Mott temperature in the PNJL and the conventional NJL models.

In Fig. 8, we show the calculated results of the  $s$ -wave  $\pi$ - $\pi$  scattering lengths  $a_0$  and  $a_2$  as functions of the temperature in unit of  $T_M$  in the PNJL model with two Polyakov-loop effective potentials and in the conventional NJL model. Since  $a_0$  and  $a_2$  contain contribution from the  $T$ -matrix amplitude  $T_c$  as Eq. (61) shows, they are both divergent at  $T = T_M$ . Furthermore,  $a_0$  also contains  $T_d$ , so it diverges at  $T = T_d^\sigma$  as well. At zero temperature, we have  $a_0 = 0.173$  and  $a_2 = -0.045$ , which are consistent with the Weinberg values  $(a_0)^W = 7m_\pi^2/(32\pi f_\pi^2) = 0.158$  and  $(a_2)^W = -2m_\pi^2/(32\pi f_\pi^2) = -0.045$  [64, 66]. On the experimental side, the Geneva-Saclay collaboration provided the often quoted values  $a_0 = 0.26 \pm 0.05$  and  $a_2 = -0.028 \pm 0.012$  [68, 69], and recent years experiment E865 at Brookhaven National Laboratory, USA, has given new values  $a_0 = 0.203 \pm 0.033 \pm 0.004$  and  $a_2 = -0.055 \pm 0.023 \pm 0.003$  [70], and also  $a_0 = 0.216 \pm 0.013 \pm 0.004 \pm 0.005$  [71]. The scattering lengths  $a_0$  and  $a_2$  are almost independent of the temperature until the temperature is increased to  $0.9T_M$  in the PNJL model, and after that they vary drastically with temperature. While in the conventional NJL model  $a_0$  and  $a_2$  begin to vary with temperature at about  $0.6T_M$  and the temperature at which  $a_0$  diverges due to the  $\sigma$ -meson dissociation is also lower in the conventional NJL model. From the above analysis, one can recognize that the physical meaning of the divergence of the  $s$ -wave  $\pi$ - $\pi$  scattering lengths  $a_0$  and  $a_2$  at the Mott

temperature  $T_M$  for  $\pi$  meson is clear and consistent with that shown in Ref. [64]. At  $T = T_M$ ,  $\pi$  meson can dissociate into a constituent quark and an antiquark, the  $\pi$  meson is then unbound and its radius becomes infinite. Mathematically, the geometrical size of the pion meson can be described by its charge radius  $r$  which is related to  $f_\pi$  through  $f_\pi^2 \propto 1/\langle r^2 \rangle$  [64]. Employing the Weinberg relations cited above, we have the relation between the scattering lengths and the charge radius of  $\pi$  meson as  $|a| \propto \langle r^2 \rangle$ , which clearly indicates that the divergence of  $\pi$ - $\pi$  scattering lengths at the pion Mott temperature is closely related with the melting of the pion meson. The relation between the divergence of the  $s$ -wave  $\pi$ - $\pi$  scattering lengths and the delocalization of the pion meson at  $T_M$  is then confirmed not only in the conventional NJL model but also in the PNJL model. As for the divergence of the  $s$ -wave  $\pi$ - $\pi$  scattering length  $a_0$  at the dissociation temperature for  $\sigma$  meson  $T_d^\sigma$ , we should note that this divergence corresponds to the situation that the propagator for  $\sigma$  meson displayed in the part d of Fig. 6 is on shell, which means that the  $\pi$ - $\pi$  scattering in the  $s$  channel couples resonantly with the  $\sigma$  meson field. The divergence (from positive infinite to negative infinite) of the  $a_0$  and the mass relation  $m_\sigma = 2m_\pi$  suggest that, in general point of view, a very loosely bound state may appear at the dissociation temperature  $T_d^\sigma$ . However, detailed investigation is required to clarify its mechanism.

## 5 Summary

In summary, we have studied the mesonic excitations at finite temperature in the two flavor PNJL model. The masses of  $\pi$  meson and  $\sigma$  meson, pion-decay constant, and the pion-quark coupling strength at finite temperature are calculated in the PNJL model with two forms of Polyakov-loop effective potential. Their variation behaviors with temperature, especially when the temperature takes a value near the critical one, are investigated in details. We find that the results calculated in the PNJL model are almost independent of the choice of the Polyakov-loop effective potential. We also compare our calculated results in the PNJL model with those in the conventional NJL model. We find that, since in the PNJL model, the Polyakov-loop which is coupled with quarks suppresses the unwanted degrees of freedom below the critical temperature, all quantities describing the properties of mesons deviate from their values at zero temperature only when the temperature is very near the critical temperature, for example the Mott temperature, and they vary with temperature rapidly in a very narrow region near the critical one. While in the conventional NJL model, these quantities begin to vary with temperature much earlier. Therefore, we conclude that the effect of color confinement screens the effect of temperature below the critical temperature. Furthermore, we have investigated the Goldberger-Treiman relation and the Gell-Mann–

Oakes–Renner relation at finite temperature in the PNJL model, and we find that when the temperature is below about  $0.9T_M$ , where  $T_M$  is the Mott temperature for  $\pi$  meson, these two important relations are hardly changed by the effect of temperature. However, the Goldberger–Treiman relation and the Gell-Mann–Oakes–Renner relation should be corrected once the temperature is in the region of  $0.9T_M \sim T_M$ .

In this work, we have also investigated the  $s$ -wave  $\pi$ – $\pi$  scattering lengths at finite temperature in the PNJL model. The obtained results in the PNJL model are also compared with those in the conventional NJL model. We find that scattering length  $a_0$  is divergent at Mott temperature for  $\pi$  meson,  $T_M$ , and at dissociation temperature for  $\sigma$  meson,  $T_d^\sigma$ , and scattering length  $a_2$  is divergent at  $T_M$ , which are consistent with the results in the conventional NJL model. Due to the effect of color confinement, the dissociation temperature for  $\sigma$  meson  $T_d^\sigma$  calculated in unit of  $T_M$  in the PNJL model is relatively larger than that given in the conventional NJL model. In the same way, the influence of the temperature on the scattering lengths  $a_0$  and  $a_2$  below the critical temperature is suppressed by the color confinement in the PNJL model. In addition, the characteristic of the scattering amplitude  $T_a$  at the Mott temperature calculated in the PNJL model is different from that given previously in the conventional NJL model.

## Acknowledgements

This work was supported by the National Natural Science Foundation of China under contract No. 10425521 and No. 10675007, and the Major State Basic Research Development Program under contract No. G2007CB815000. Helpful discussions with Dr. Craig D. Roberts at Argonne National Laboratory, USA, and Prof. Chuan Liu, Prof. Han-qing Zheng and Dr. Lei Chang are acknowledged with great thanks.

## References

- [1] E. V. Shuryak, Prog. Part. Nucl. Phys. **53**, 273 (2004).
- [2] M. Gyulassy, and L. McLerran, Nucl. Phys. A **750**, 30 (2005).
- [3] E. V. Shuryak, Nucl. Phys. A **750**, 64 (2005).
- [4] I. Arsene *et al*, Nucl. Phys. A **757**, 1 (2005).
- [5] B. B. Back *et al*, Nucl. Phys. A **757**, 28 (2005).
- [6] J. Adams *et al*, Nucl. Phys. A **757**, 102 (2005).
- [7] K. Adcox *et al*, Nucl. Phys. A **757**, 184 (2005).
- [8] J.-P. Blaizot, J. Phys. G **34**, S243 (2007).
- [9] F. Weber, Prog. Part. Nucl. Phys. **54**, 193 (2005).
- [10] M. Alford, D. Blaschke, A. Drago, T. Klähn, G. Pagliara, J. Shaffner-Bielich, Nature **445**, E 7 (2007).
- [11] M. Alford, A. Schmitt, K. Rajagopal, and T. Schäfer, Rev. Mod. Phys. **80**, 1455 (2008).
- [12] W. J. Fu, H. Q. Wei, and Y. X. Liu, Phys. Rev. Lett. **101**, 181102 (2008).
- [13] P. Costa, M. C. Ruivo, C. A. de Sousa, and Y. L. Kalinovsky, Phys. Rev. D **70**, 116013 (2004); Phys. Rev. D **71**, 116002 (2005).
- [14] H. Hansen, W. M. Alberico, A. Beraudo, A. Molinari, M. Nardi, and C. Ratti, Phys. Rev. D **75**, 065004 (2007).
- [15] P. Costa, M. C. Ruivo, C. A. de Sousa, H. Hansen, and W. M. Alberico, arXiv:0807.2134[hep-ph].
- [16] Y. Nambu, and G. Jona-Lasinio, Phys. Rev. **122**, 345 (1961); Phys. Rev. **124**, 246 (1961).
- [17] M. K. Volkov, Ann. Phys. **157**, 282 (1984).
- [18] S. P. Klevansky, Rev. Mod. Phys. **64**, 649 (1992).
- [19] T. Hatsuda, and T. Kunihiro, Phys. Lett. B **145**, 7 (1984); Phys. Rep. **247**, 221 (1994).
- [20] R. Alkofer, H. Reinhardt, and H. Weigel, Phys. Rep. **265**, 139 (1996).

- [21] M. Buballa, Phys. Rep. **407**, 205 (2005).
- [22] P. N. Meisinger, and M. C. Ogilvie, Phys. Lett. B **379**, 163 (1996); P. N. Meisinger, T. R. Miller, and M. C. Ogilvie, Phys. Rev. D **65**, 034009 (2002).
- [23] R. D. Pisarski, Phys. Rev. D **62**, 111501(R) (2000); A. Dumitru and R. D. Pisarski, Phys. Lett. B **504**, 282 (2001); Phys. Lett. B **525**, 95 (2002); Phys. Rev. D **66**, 096003 (2002).
- [24] K. Fukushima, Phys. Lett. B **591**, 277 (2004).
- [25] Á. Mócsy, F. Sannino, and K. Tuominen, Phys. Rev. Lett. **92**, 182302 (2004).
- [26] E. Megías, E. Ruiz Arriola, and L.L. Salcedo, Phys. Rev. D **74**, 065005 (2006); Phys. Rev. D **74**, 114014 (2006).
- [27] C. Ratti, M. A. Thaler, and W. Weise, Phys. Rev. D **73**, 014019 (2006).
- [28] S. Rößner, C. Ratti, and W. Weise, Phys. Rev. D **75**, 034007 (2007).
- [29] W. J. Fu, Z. Zhang, and Y. X. Liu, Phys. Rev. D **77**, 014006 (2008).
- [30] M. Ciminale, R. Gatto, N. D. Ippolito, G. Nardulli, and M. Ruggieri, Phys. Rev. D **77**, 054023 (2008).
- [31] S. K. Ghosh, T. K. Mukherjee, M. G. Mustafa, and R. Ray, Phys. Rev. D **73**, 114007 (2006).
- [32] C. Ratti, S. Rößner, M. A. Thaler, and W. Weise, Eur. Phys. J. C **49**, 213 (2007).
- [33] Z. Zhang, and Y. X. Liu, Phys. Rev. C **75**, 064910 (2007).
- [34] C. Sasaki, B. Friman, and K. Redlich, Phys. Rev. D **75**, 074013 (2007).
- [35] C. Ratti, S. Rößner, and W. Weise, Phys. Lett. B **649**, 57 (2007).
- [36] S. K. Ghosh, T. K. Mukherjee, M. G. Mustafa, and R. Ray, Phys. Rev. D **77**, 094024 (2008).
- [37] H. Abuki, M. Ciminale, R. Gatto, N. D. Ippolito, G. Nardulli, and M. Ruggieri, Phys. Rev. D **78**, 014002 (2008).
- [38] T. Kähärä, and K. Tuominen, Phys. Rev. D **78**, 034015 (2008).

- [39] H. Abuki, R. Anglani, R. Gatto, G. Nardulli, and M. Ruggieri, Phys. Rev. D **78**, 034034 (2008).
- [40] K. Kashiwa, H. Kouno, M. Matsuzaki, and M. Yahiro, Phys. Lett. B **662**, 26 (2008).
- [41] P. Costa, C. A. de Sousa, M. C. Ruivo, and H. Hansen, arXiv:0801.3616 [hep-ph].
- [42] K. Fukushima, Phys. Rev. D **78**, 114019 (2008).
- [43] G. A. Contrera, D. G. Dumm, and N. N. Scoccola, Phys. Lett. B **661**, 113 (2008).
- [44] K. Fukushima, Phys. Rev. D **77**, 114028 (2008).
- [45] S. Mukherjee, M. G. Mustafa, and R. Ray, Phys. Rev. D **75**, 094015 (2007).
- [46] B. Hiller, J. Moreira, A.A. Osipov, and A.H. Blin, arXiv:0812.1532[hep-ph]
- [47] M. Ciminale, R. Gatto, G. Nardulli, and M. Ruggieri, Phys. Lett. B **657**, 64 (2007).
- [48] H. Abuki, M. Ciminale, R. Gatto, G. Nardulli, and M. Ruggieri, Phys. Rev. D **77**, 074018 (2008).
- [49] D. Gomez Dumm, D.B. Blaschke, A.G. Grunfeld, and N.N. Scoccola, Phys. Rev. D **78**, 114021 (2008).
- [50] D. Blaschke, M. Buballa, A. E. Radzhabov, and M. k. Volkov, Yad. Fiz. **71**, 2012 (2008) [Phys. At. Nucl. **71**, 1981 (2008)].
- [51] S. Rößner, T. Hell, C. Ratti, and W. Weise, Nucl. Phys. A **814**, 118 (2008).
- [52] Y. Sakai, K. Kashiwa, H. Kouno, and M. Yahiro, Phys. Rev. D **77**, 051901(R) (2008).
- [53] Y. Sakai, K. Kashiwa, H. Kouno, and M. Yahiro, Phys. Rev. D **78**, 036001 (2008).
- [54] K. Kashiwa, Y. Sakai, H. Kouno, M. Matsuzaki, and M. Yahiro, arXiv:0804.3557 [hep-ph].
- [55] Y. Sakai, K. Kashiwa, H. Kouno, M. Matsuzaki, and M. Yahiro, Phys. Rev. D **78**, 076007 (2008).
- [56] K. Dusling, C. Ratti, and I. Zahed, Phys. Rev. D **79**, 034027 (2009).
- [57] B. Mueller, arXiv:0812.4638 [nucl-th].
- [58] K. Fukushima, arXiv:0901.0783 [hep-ph].



- [59] M. L. Goldberger, and S. B. Treiman, Phys. Rev. **110**, 1178 (1958).
- [60] M. Gell-Mann, R. Oakes, and B. Renner, Phys. Rev. **175**, 2195 (1968).
- [61] O. Kaczmarek, F. Karsch, P. Petreczky, and F. Zantow, Phys. Lett. B **543**, 41 (2002).
- [62] G. Boyd, J. Engels, F. Karsch, E. Laermann, C. Legeland, M. Lügemeier, and B. Petersson, Nucl. Phys. B **469**, 419 (1996).
- [63] H. J. Schulze, J. Phys. G. **21**, 185 (1995).
- [64] E. Quack, P. Zhuang, Y. Kalinovsky, S. P. Klevansky and J. Hüfner, Phys. Lett. B **348**, 1 (1995).
- [65] P. Maris, C. D. Roberts, S. M. Schmidt, and P. C. Tandy, Phys. Rev. C **63**, 025202 (2001).
- [66] V. Bernard, U-G. Meißner, A. H. Blin and B. Hiller, Phys. Lett. B **253**, 443 (1991).
- [67] V. Bernard, A. A Osipov, and U-G. Meißner, Phys. Lett. B **285**, 119 (1992).
- [68] C. D. Froggatt, and J. L. Petersen, Nucl. Phys. B **129**, 89 (1977).
- [69] M. M. Nagels *et al.*, Nucl. Phys. B **147**, 189 (1979).
- [70] P. Truöl, arXiv:hep-ex/0012012.
- [71] S. Pislak *et al.*, Phys. Rev. Lett. **87**, 221801 (2001).